Int J Earth Sci (Geol Rundsch) (2008) 97:115–134
DOI 10.1007/s00531-006-0166-7

ORIGINAL PAPER

Integrated stratigraphy and $^{40}Ar/^{39}Ar$ chronology of the Early to Middle Miocene Upper Freshwater Molasse in eastern Bavaria (Germany)

H. Abdul Aziz · M. Böhme · A. Rocholl · A. Zwing · J. Prieto · J. R. Wijbrans · K. Heissig · V. Bachtadse

Received: 11 August 2006 / Accepted: 17 December 2006 / Published online: 25 January 2007

Abstract A detailed integrated stratigraphic study was carried out on middle Miocene fluvial successions of the Upper Freshwater Molasse (OSM) from the North Alpine Foreland Basin, in eastern Bavaria, Germany. The biostratigraphic investigations yielded six new localities thereby refining the OSM biostratigraphy for units C to E (sensu; Heissig, Actes du Congres BiochroM'97. Mem Trav EPHE, Inst Montpellier 21, 1997) and further improving biostratigraphic correlations between the different sections throughout eastern Bavaria. Radioisotopic ages of 14.55 ± 0.19 and 14.88 ± 0.11 Ma have been obtained for glass shards from the main bentonite horizon and the Ries impactite: two important stratigraphic marker beds used for confirming our magnetostratigraphic calibration to the Astronomical Tuned Neogene Time Scale (ATNTS04; Lourens et al. in Geologic Time Scale 2004, Cambridge University Press, 2004). Paleomagnetic analysis was performed using alternating field (AF) and thermal (TH) demagnetization methods. The AF method revealed both normal and reverse polarities but proofs to yield unreliable ChRM directions for the Puttenhausen section. Using the biostratigraphic information and radioisotopic ages, the magnetostratigraphic records of the different sections are tentatively correlated to the Astronomical Tuned Neogene Time Scale (ATNTS04; Lourens et al. in Geologic Time Scale 2004, Cambridge University Press, 2004). This correlation implies that the main bentonite horizon coincides to chron C5ADn, which is corroborated by its radioisotopic age of 14.55 Ma, whereas the new fossil locality Furth 460, belonging to OSM unit E, probably correlates to chron C5Bn.1r. The latter correlation agrees well with the Swiss Molasse locality Frohberg. Correlations of the older sections are not straightforward. The Brock horizon, which comprises limestone ejecta from the Ries impact, possibly correlates to C5ADr (14.581–14.784 Ma), implying that, although within error, the radioisotopic age of 14.88 ± 0.11 Ma is somewhat too old. The fossil localities in Puttenhausen, belonging to

Electronic supplementary material The online version of this article (doi: 10.1007/s00531-006-0166-7) contains supplementary material, which is available to authorized users.

H. Abdul Aziz (✉) · V. Bachtadse
Department for Earth and Environmental Sciences, Section Geophysics, Ludwig-Maximilians-University Munich, Theresienstrasse 41, 80333 Munich, Germany
e-mail: haziz@geophysik.uni-muenchen.de

M. Böhme · J. Prieto
Department for Earth and Environmental Sciences, Section Palaeontology, Ludwig-Maximilians-University Munich, Richard-Wagner-Str. 10, 80333 Munich, Germany

A. Rocholl
Department for Earth and Environmental Sciences, Section Mineralogy, Ludwig-Maximilians-Universität München, Theresienstrasse 41, 80333 Munich, Germany

K. Heissig
Bavarian State Collection for Palaeontology and Geology Munich, Richard-Wagner-Str. 10, 80333 Munich, Germany

J. R. Wijbrans
Department of Isotope Geochemistry, Vrije Universiteit Amsterdam, De Boelelaan 1085, 1081 HV Amsterdam, The Netherlands

A. Zwing
Ludwig-Maximilians-University Munich, Leopoldstrasse 3, 80802 Munich, Germany

the older part of OSM unit C, probably coincide with chron C5Cn.2n or older, which is older than the correlations established for the Swiss Molasse.

Keywords Biostratigraphy · Magnetostratigraphy · $^{40}Ar/^{39}Ar$ dating · Middle Miocene · Molasse

Introduction

The Molasse Basin is a classical foreland basin situated at the northern margin of the Alps and has been the subject of numerous studies focusing on facies distribution, stratigraphic, sedimentological and structural evolution of the basin and its response to the tectonic history of the orogenic wedge (Schlunegger et al. 2002; Kuhlemann et al. 2002; Kuhlemann and Kempf 2002; and references therein). Although a detailed (micro)-mammal biostratigraphy has been established for Miocene deposits of the Molasse Basin (Heissig 1997; Böhme et al. 2002) it does not provide a precise temporal resolution necessary for establishing a causal link between the stratigraphic record of the Molasse Basin and the tectonic evolution of the Alps as well as global climate change. Recent studies in the Swiss part of the Molasse Basin have successfully established a detailed magnetostratigraphic and biostratigraphic framework for Oligocene to Middle Miocene sequences (Schlunegger et al. 1996; Kempf et al. 1997, 1999). Conversely, the central and eastern part of the Molasse Basin in southern Germany, well known for its vast amount of sedimentological and paleontological as well as paleoclimatological information, lacks a reliable time-stratigraphic framework. This especially holds for the Early to Late Miocene Upper Freshwater Molasse of the Bavarian part of the Molasse Basin, which is one of the richest and most densely sampled Neogene basins of Europe with over more than 200 vertebrate and paleobotanical localities.

In this paper, we present a chronostratigraphic framework for different surface outcrops in the eastern part of Bavaria using an integrated biostratigraphic, magnetostratigraphic and radiometric approach. We include results of the 2004 paleomagnetic and biostratigraphic fieldwork season, advances in the biostratigraphic subdivision, and results of radioisotopic dating of the two important stratigraphic tie-points: the Ries event and the main bentonite horizon. Our integrated stratigraphic approach is a first attempt to calibrate the existing biostratigraphic record to the new Astronomically Tuned Neogene Time Scale (ATNTS04, Lourens et al. 2004). This approach will allow establishing correlations between continental sequences throughout the Molasse Basin, creating a link to global climate change and the tectonic evolution of the Alps, and contribute to improved biostratigraphic correlations across European Neogene basins. Moreover, it will provide the chronologic framework necessary to address key-issues related to mammal evolution and migration rates for Central and Western Europe.

Geological setting

The Molasse Basin, also known as the Northern Alpine Foreland Basin (NAFB), extends about 1,000 km along the Alpine front from Lake Geneva in the west to the eastern termination of the Alps in Austria (Fig. 1). During the Cenozoic, the NAFB was formed as a mechanical response to the tectonic load of the evolving Alps (e.g., Homewood et al. 1986; Schlunegger et al. 1997) causing a flexural bulge in the European lithosphere, which acted as a sediment sink for the erosional debris of the uplifting Alps. The sedimentary facies of the Molasse is characterized by a pronounced temporal and lateral variability with radial alluvial fan sedimentation in the southern part of the basin and E-W fluvial alluvial sedimentation more northward along the basin axis. Two long-term sedimentary cycles, reflected by a repetitive change from marine to terrestrial sedimentary environments, dominate the Molasse sequences and are, accordingly, subdivided into Lower Marine/Freshwater Molasse (UMM/USM) and Upper Marine/Freshwater Molasse (OMM/OSM) (Bachmann and Müller 1991; Reichenbacher et al. 1998).

In eastern Bavaria (Fig. 1), the Upper Freshwater Molasse (Obere Süßwasser Molasse, OSM) can be divided lithostratgraphically into *limnische Süßwasserschichten, fluviatile Süßwasserschichten, Nördlicher Vollschotter* (NV) and *Hangendserie* (Wurm 1937; Batsche 1957; Hofmann 1973; Doppler et al. 2000). Our studied sections in the Mainburg and Landshut area (Fig. 1) all belong to the NV lithostratigraphic unit (Fig. 2). This NV is subdivided into two parts separated by the *Süßwasserkalk* (SK) (Batsche 1957) and typically consists of coarse grained and poorly sorted gravels. The lower part of the NV is generally coarser (maximum gravel size 22–25 cm) and is overlain by the SK unit, which comprises an up to 10 m thick, typically strongly calcareous paleosol horizon. The upper part of the NV comprises in the Landshut area several paleosol horizons, which show a relatively continuous distribution over several tens of kilometers (Batsche 1957; Herold 1970; Hofmann 1973). The

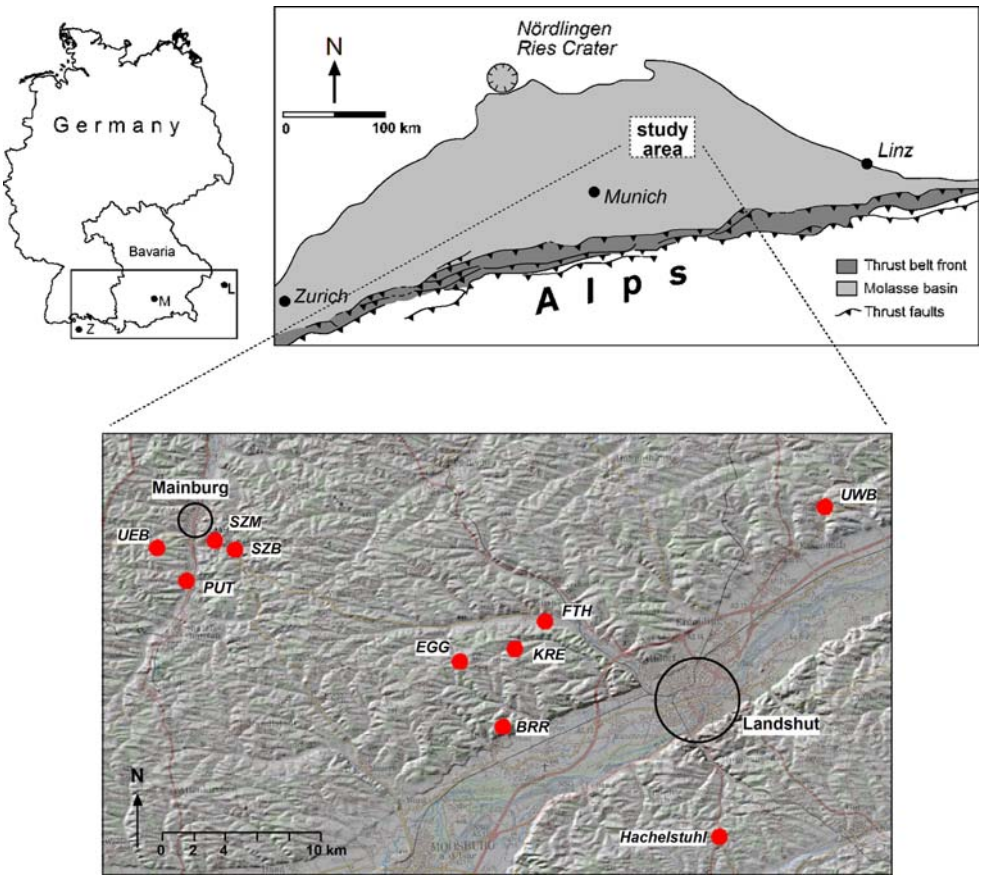

Fig. 1 Location maps of study area and sections, and sketch map of Molasse Basin

stratigraphically uppermost paleosol corresponds to the ~7 m thick *Zwischenmergel* (ZM, Hofmann 1973). The base of the gravel unit above the ZM contains Jurassic limestone boulders of the Ries impact (Brock horizon) and can be found in several sections in the study area, (e.g., Kreut section, Enghausen, Wachelkofen; Ulbig 1994). Finally, the uppermost gravel-horizon of the NV, usually deeply weathered (Herold 1970), is overlain by 5–7 m thick fine-grained, marly sediments of the Sand-Mergel-Decke (SMD). In this unit, an up to 3 m thick tuff horizon occurs: the main-bentonite layer of eastern Bavaria.

Biozonations

The first biozonation of the OSM deposits was given by Dehm (1955), who introduced the terms Older, Middle and Younger Series, defined respectively by the absence of deinotherid proboscidians, the presence of the small sized *Prodeinotherium bavaricum* and the presence of the large sized *Deinotherium giganteum*. Later, Fahlbusch (1964), Heissig (1990) and Boon (1991) proposed a biozonation for the Older and Middle Series based on cricetid (hamsters) evolutionary stages and successions of small mammal communities. For the Older and Middle Series, Heissig (1997) introduced six faunal units (OSM A–OSM F) and a corresponding cyclostratigraphy of 11 fining upward cyclothems (OSM 0–OSM 10). Each cyclothem is defined (following Scholz 1986) by a course, gravely and sandy fluvial unit at the base and a fine-grained floodplain or pedogenic unit at the top. The faunal units OSM A to OSM D correspond to the Older series, whereas the units OSM E to OSM F correspond to the Middle series. Both series are separated by an erosional hiatus, the pre-Riesian hiatus of Birzer (1969). The most recent stratigraphical update was given by Böhme et al. (2002) who defined a new faunal unit OSM E' between OSM E and OSM F.

Sections and correlations

Relative lithostratigraphic correlations between the studied sections (Fig. 2) are established using one or more of the following important stratigraphic markers: vertebrate fossil localities, the main bentonite layer and the Brock horizon of the Ries impact.

The Puttenhausen section comprises an 18 m thick succession of fine-grained alluvial deposits (Fig. 2).

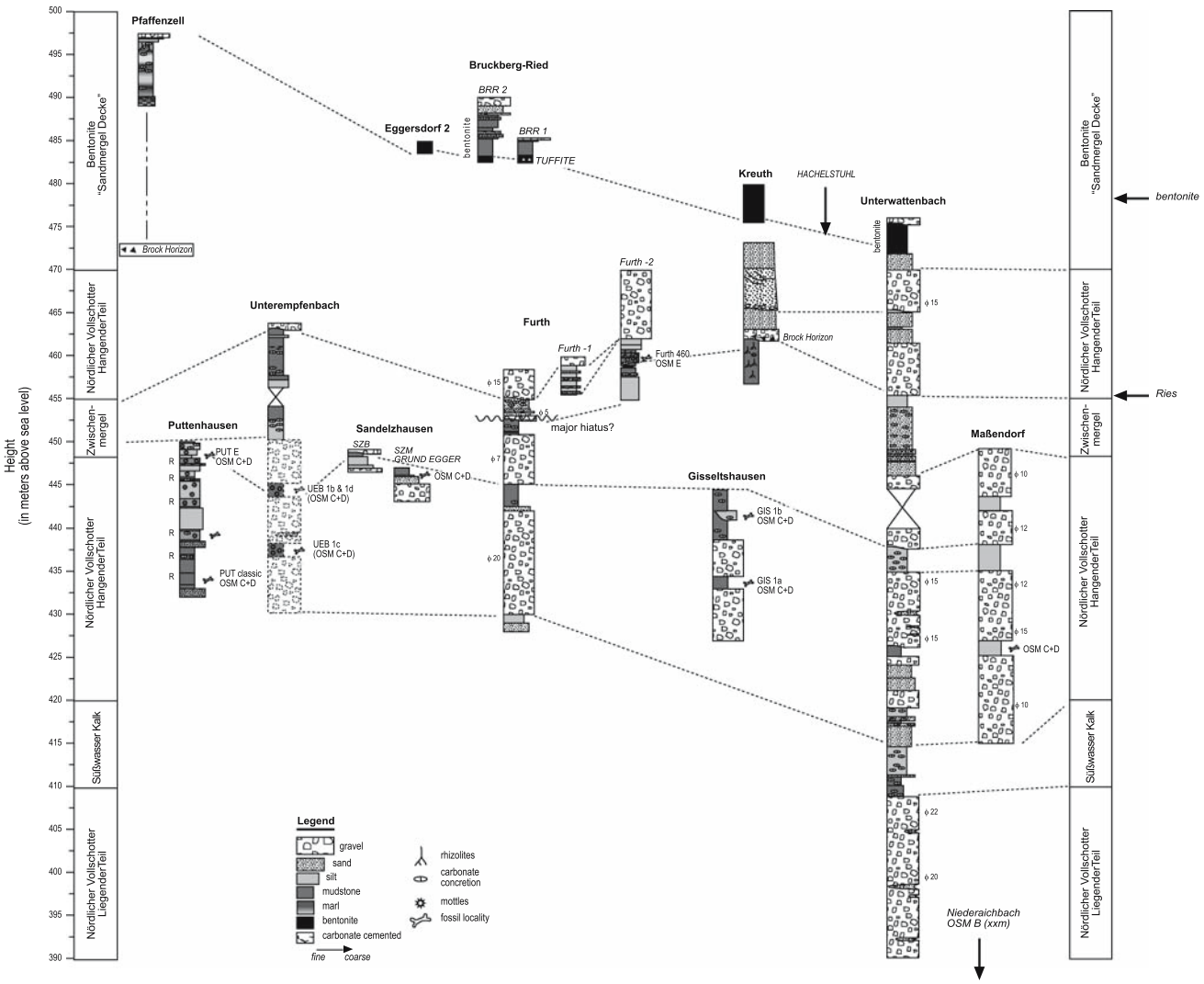

Fig. 2 Lithostratigraphic subdivision (Hofmann 1973) of the eastern Bavarian Molasse and correlation between studied sections. Fossil sites with their corresponding OSM unit are indicated. In the Puttehausen section, *R* indicates red paleosol. The sections are positioned according to their topographic height

The sediments show a cyclic alternation of blue–grey and dark–red colors, which are indicative of intense pedogenetic processes (rubified calcic pseudogleysol after Schmid 2002). At least six red paleosols rich in fossil vertebrates (our new Puttenhausen localities A to E) are recognized. The lowermost horizon contains the classic Puttenhausen fossil level of Fahlbusch and Wu (1981). Laterally, a thick fluvial channel cuts into the cyclic paleosol profile.

The famous Sandelzhausen fossil locality (Fahlbusch et al. 1972), a gravel pit of the Karger Co. (acronym SZA) is abandoned since 2004. The Sandelzhausen (SZ) section sampled for this study corresponds to the fossil-bearing layers of SZA (Fig. 2). The section is situated on top of gravels of the NV and contains 2.5 m thick moderate to weakly pedogenized gravelly marls (base), marls and clays (top) with well developed calcrete horizons. Several hundreds of meters from Sandelzhausen, two other outcrops have also been studied: one to the east (Sandelzhausen gravel pit, Beck Co., acronym SZB) and the other to the west (Sandelzhausen former gravel pit Mitterfeld, acronym SZM). The lithologic characteristics and relative topographic position of these sections enable a correlation to the SZA section.

Only the uppermost part of the Unterempfenbach gravel pit [448–465 m above mean sea level (amsl)] was temporarily exposed in 2004 (Fig. 2). The lower part of the section, currently inaccessible, contains gravels of the NV (Gregor 1969; Heissig personal observations). The vertebrate fauna of Unterempfenbach 1c was found in a gastropod rich, pedogenic horizon at around

438 m amsl. This horizon is followed by limnic marls and a paleosol containing the vertebrate faunas of Unterempfenbach 1b and 1d. The upper part of the section consists of intensively pedogenized fine-grained alluvial sediments, intercalated with calcrete horizons. The top of this pseudogleysol is slightly rubified and is erosively overlain by sandy gravels.

The 42 m thick Furth section (Fig. 2) consists of five successive fining-up cyclothems each beginning, except the last one, with coarse, grey colored carbonate rich gravels (gravel diameter up to 20 cm, typical for the NV) and ending with fine grained floodplain sediments. The three lower fine-grained cyclothems are weakly pedogenized. The fourth one (~10 m thick) is intensively pedogenized with a partly rubified calcic pseudogleysol on the top. This paleosol, labeled Furth-2 section in this study, correlates to the ZM and in the top part contains a new fossil locality (Furth 460 m). Laterally, the paleosol is eroded by a steep E-W oriented channel consisting of sandy sediments (Furth-1 section) with numerous reworked carbonate concretions at the base. Hence, Furth 1 lies stratigraphically above Furth 2. The uppermost gravel of the last cyclothem is yellowish and rusty colored. The gravels show similar lithological characteristics as the gravels in the Kreut section (2 km southwest of Furth section; see below), which contains at the base Ries impact boulders (Brock horizon).

The sand and gravel pit at Kreut is situated 2 km southwest of the Furth section. The base of the section consists of pedogenically overprinted (rhizocrete), laminated lacustrine marls (Fig. 2). These marls are erosively overlain by 3 to 4 m thick yellowish to brownish carbonate-free coarse gravels and 1.5 m sand. Locally, the base of these gravels contains up to 10 cm large angular Late Jurassic limestone boulders, originating from the Ries impact (Brock horizon, Böhme et al. 2002). These sediments are subsequently erosively overlain by several meters of coarse gravels containing reworked calcretes and up to 10 m of large-scale cross-bedded sands. One kilometer south of Kreut, the main bentonite layer was historically exposed at a height of 475–480 m NN, which is stratigraphically above the Kreut section (Ulbig 1994).

The base of the 85 m thick Unterwattenbach section contains gravels rich in carbonate pebbles (maximum diameter 22 cm), which are characteristic for the top of the lower part of the NV (Fig. 2). Above these sediments, between 409 and 419 m, a heavily pedogenized white to bluish marl is exposed, comprising three to four pedogenic cycles. This marl could correlate to the SK. In the subsequent gravel interval (maximum pebble diameter 15 cm), fine-grained sediments containing partly eroded sands and clays and pedogenized green marls occur. The gravel interval is followed by 2.5 m of fine sands and 4.5 m of a green, pedogenized marls, which correlate to the ZM. The transition to the overlying gravels is not well exposed. The top part of the Unterwattenbach section comprises a 6 m thick fining up (from middle sand to silty clay) unit, which correlates to the SMD and the (reworked) main bentonite horizon. This interval is finally erosively overlain by gravels.

The only section studied in the Augsburg area is the gravel and sand pit of Pfaffenzell. In Pfaffenzell, post-Riesian sediments, including the Brock horizon at the base of the profile (about 30 m below out measured section), are exposed. At the northern end of the gravel pit, near the village Pfaffenzell-Weiler, the top of the profile crops out. This profile comprises 10 m thick fine to coarse gravels (Gallenbacher Schotter of Fiest 1989), followed by ~7 m of fine-sandy silts (Sand-Mergel-Abfolge of Fiest 1989). In our studied Pfaffenzell-Weiler section, an erosional depression is found on the top of this silt unit and comprises 6 m thick laminated, dark bituminous and blue grey lacustrine marls and about 2 m of yellowish marls and silt with a weak pedogenic overprint. About 150 m east of our section, the main bentonit layer is found at a topographic height of 515 m.

The bentonite pits of the Bruckberg-Ried and Eggersdorf sections belong to the SMD and are similar to the sedimentary cycle of Pfaffenzell-Weiler. Both sections contain the main bentonite layer with their overlying fine-grained sediments. The base of these sections contains an up to 3 m thick consolidated, relatively fresh whitish tuff, which is subsequently followed by 2 m of industrially excavated high-quality bentonite and up to 3 m of reworked bentonite or sandy clays.

Biostratigraphy

In the NAFB the biostratigraphy is based on evolutionary succession of small-mammal assemblages (Fig. 3). Following Heissig (1997) and Böhme et al. (2002), the regional faunal unit OSM A is characterized by the presence of the genera *Ligerimys florancei* and the very small sized *Megacricetodon* aff. *collongensis*. Faunal unit OSM B contains no *Ligerimys* but is defined by the First Appearance Date (FAD) of *Keramidomys* and *Megacricetodon bavaricus*, the latter evolving from *M.* aff. *collongensis*. The younger faunal unit OSM C + D is characterized by a further size increase of *Megacricetodon* (*M.* aff. *bavaricus*) and the

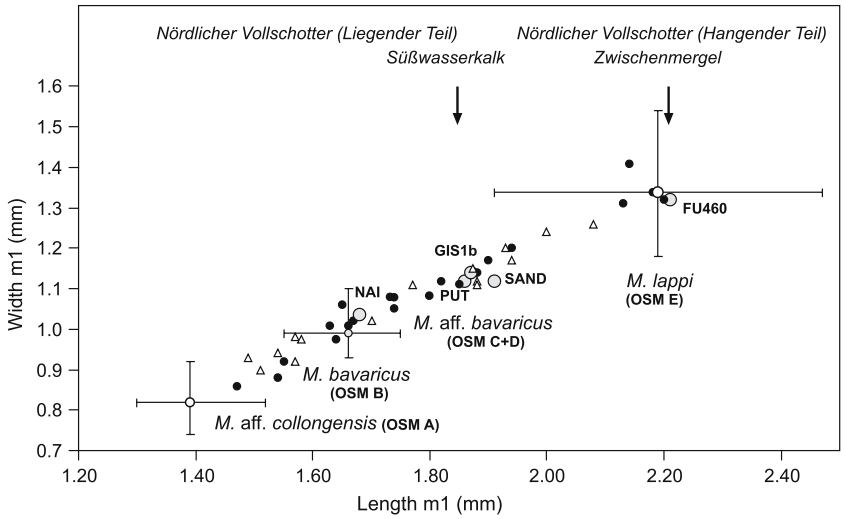

Fig. 3 Size increase of *Megacricetodon* m1 molar from OSM A to OSM E. *Large grey dots* represent samples from the eastern Bavarian Molasse (*SAND* Sandelzhausen, *PUT* Puttenhausen, *GIS1b* Gisseltshausen 1b and *NAI* Niederaichbach), *black dots* (white triangles) from the German (Swiss) Molasse and *open circles* are samples from Vieux Collonges (France). The scatter range is indicated for the type localities Vieux Collonges (*M. collongensis*, *M. lappi*) and Langenmoosen (*M. bavaricus*, *grey dot*). *Arrows* indicate the position of the two fine-grained horizons Süßwasserkalk and Zwischenmergel. Measurements for all samples are listed in ''Appendix''

FAD of a small size *M.* cf. *minor* (in the later part of this unit). In contrast to Heissig (1997) and Böhme et al. (2002), we unified faunal unit OSM C and D. The characteristic species of OSM D was defined as *Anomalomys minutus*. This very rare species is known from only two localities in the NAFB, Gisseltshausen 1a (Lower Bavaria, see Fig. 2) and Tobel-Hombrechtikon (Switzerland, type locality, Bolliger 1992). Gisseltshausen 1a is superposed by Gisseltshausen 1b, which contains a *M.* aff. *bavaricus* in the size-range of Puttenhausen classic (see ''Appendix''). In contrast, Puttenhausen classic contains *Anomalomys minor* (Table 1). At this moment we assume that *A. minutus* (which differ from *A. minor* only in 10% reduced size, Bolliger 1992) lived contemporary with *A. minor* in the NAFB. Faunal unit OSM E is defined by the FAD and LAD (Last Appearance Date) of *Megacricetodon lappi* and *Cricetodon meini* and a *M. minor* of typical size whereas in OSM E' *M.* aff. *lappi* is replaced by the immigrant *M.* aff. *gersi*. Finally, OSM F is characterized by the FAD of *Cricetodon* aff. *aureus* and *Anomalomys gaudryi*.

The oldest studied lithostratigraphic unit, the lower part of NV in the Unterwattenbach section, contains no fossils. The only biostratigraphic useful fauna for the lower part of NV comes from Niederaichbach 4.5 km SE of Unterwattenbach section. The fauna contains a typical sized *Megacricetodon bavaricus* and could thus correlate to the fauna of Langenmoosen and Bellenberg (Schötz 1993), corresponding to faunal unit OSM B.

Puttenhausen section

The six red soil horizons have produced rich microvertebrate assemblages (PUT A to E). The lowermost sample PUT A correlates to the classical Puttenhausen fauna (Fahlbusch and Wu 1981; Wu 1982, 1990; Ziegler and Fahlbusch 1986; Ziegler 2000, 2005). The presence of the larger sized *Megacricetodon* aff. *bavaricus* suggests that both samples belong to faunal unit OSM C + D. Because of the evolutionary stage of *Megacricetodon* and *Miodyromys*, these samples are considered to be older than the Sandelzhausen assemblage (Fig. 3).

The faunal assemblages found in PUT B to PUT D show no significant difference to PUT A or the classical level (Fig. 3, Table 1), although the biostratigraphic important large *Megacricetodon* species is rare in all samples. However, PUT E (445.5–448 m) yielded two m/2 of a small *Megacricetodon* cf. *minor*, which are smaller than the rare small *Megacricetodon* from PUT classic (Wu 1982) and similar in size to *M.* cf. *minor* found in Sandelzhausen [Fahlbusch 1964; Wessels and Reumer 2006 (personal communication)]. Also the presence of *Galerix aurelianensis-stehlini* in PUT E as well as in Sandelzhausen supports a younger level within OSM C + D unit. This species is absent in older levels but present in Sandelzhausen (Ziegler 2000) and in Maßendorf (Schötz 1988; the Maßendorf fossil level situated in the upper part of NV, Fig. 2), both belonging to a later part of OSM C. In addition,

Table 1 Herpeto- and small mammal fauna of the localities Puttenhausen (PUT cl.-classic, PUT A to E), Sandelzhausen (SAND), and Furth 460 m (FU 460)

		PUT cl.	PUT A	PUT B	PUT C	PUT D	PUT E	SAND	FU460
Cricetidae	*Megacricetodon* aff. *bavaricus*								
	Megacricetodon lappi								
	Megacricetodon cf. *minor*								
	Democricetodon gracilis								
	Democricetodon mutilus								
	Democricetodon sp.								
	Eumyarion bifidus								
	Eumyarion cf. *weinfurteri*								
	Neocometes sp.								
Anomalomyidae	*Anomalomys minor*								
Eomyidae	*Keramidomys thaleri*						?		sp.
Gliridae	*Microdyromys complicatus*								
	Microdyromys koenigswaldi								
	Glirulus diremptus								
	Prodryomys satus								
	Miodyromys aegercii	aff.	aff.	aff.	aff.	aff.	aff.		
	Bransatoglis astaracensis (after Bruijn & Petruso 2005) = *B. cadeoti* (after Wu 1990: 89)								
	Glirudinus cf. *undosus*								
	Glirudinus sp.								
	"*Eomuscardinus*" aff. *sansaniensis*								
Sciuridae	*Spermophilinus besanus*								
	Paleosciurius sutteri								
	Heteroxerus aff. *rubricati*								
	Blackia miocaenica								
	Forsythia cf. *gaudryi*								
	Miopetaurista dehmi					sp.	sp.		
Castoridae	cf. *Steneofiber depereti*								
Didelphidae	*Amphiperatherium frequens*	n. ssp. aff.	?aff.	?aff.	aff.	?aff.			
Soricidae	*Dinosorex zapfei*								
	Florinia aff. *stehlini*								
	Miosorex sp. 1								
	Miosorex sp. 2								
	Lartetium dehmi	?							
	Limnoecus n. sp.								
	Soricidae indet. (several species)								
Dimylidae	*Plesiodimylus chantrei*								
	Plesiodimylus n. sp.								
	Metacordylodon aff. *schlosseri*								
Talpidae	Talpidae indet. (several species)								
	Talpidae indet. (sensu ZIEGLER 2000: 118, Plate 6, fig. 75)								
	Prosacapanus sansaniensis								
	Proscapanus sp.(small)								
	Myxomygale hutchisoni								
	Mygaela jaegeri								
	?*Urotrichus* cf. *dolichochir*								
	Talpa minuta		cf.						
Erinaceidae	*Galerix* aff. *exilis*								
	Galerix aurelianensis-stehlini								
	Lanthanotherium aff. *sansaniensis*	sp.							
	Mioechinus sp.	sp.							
Vespertilionidae	*Eptesicus* sp.								
	Myotis aff. *murinodes*								
Lagomorpha	*Prolagus oeningensis*	?							
	Prolagus crusafonti-like form	?							
	?*Amphilagus* sp.								
	Lagopsis verus								
	Lagopsis cf. *penai*	sp.							
Allocaudata	*Albanerpeton inexpectatum*								
Urodela	*Salamandra sansaniensis*						sp.		
	Chelotriton paradoxus	sp.	sp.				sp.		
	Triturus (vulgaris) sp.								
	Triturus cf. marmoratus								
Anura	*Latonia gigantea*		sp.	sp.			sp.		
	Eopelobates sp.								
	Pelobates nov.sp.		sp.	sp.					
	Pelobatinae indet.								
	Rana (ridibunda) sp.								
	Bufo cf. viridis								
Crocodylia	*Diplocynodon styriacus*								
Chelonia	*Trionyx (triunguis)* sp.								
	Clemmydopsis turnauensis								
	Mauremys sophiae		aff. sp.	aff. sp.					
	Testudo rectogularis		sp.	sp.			sp.		sp.
	Ergilemys cf. perpiniana								
	Chelonia indet.								
Iguania	*Chamaeleo caroliquarti*								
	Chamaeleo bavaricus						sp.		
Scincomorpha	*Lacerta* sp. 1								
	Lacerta sp. 2								
	Miolacerta tenuis								
	Amblyolacerta dolnicensis								
	Scincidae indet. 1								
	Scincidae indet. 2								
	Cordylidae indet.			?			?		
	Scincomorpha indet. 1								
	Scincomorpha indet. 2								
Anguimorpha	*Ophisaurus cf. spinari*		sp.	sp.					
	Pseudopus moguntinus			sp.					
	Anguis sp.								
	Anguidae indet.								
	? Varanidae indet.								
Amphisbaenidae	*Palaeoblanus* cf. *tobieni*								
	Amphisbaenidae indet.								

PUT cl. and SAND after Böhme (1999, 2003), Fahlbusch (1964, 2003), Fahlbusch and Wu (1981), Wu (1982, 1990), Ziegler and Fahlbusch (1986) and Ziegler (2000, 2005). PUT A to E and FU460 this paper. The presence of taxa is indicated in *black*

Ziegler (2000) observed that the *Dinosorex* from PUT classic is somewhat smaller than from Sandelzhausen, an observation we also recognize in the size increase of *D. zapfei* from PUT C to PUT E.

Hence we conclude that the biostratigraphic information indicates that PUT E is more closely related to Sandelzhausen than to PUT classic.

Furth section

The biostratigraphic position of the Furth 460 m locality can be fixed to the faunal unit OSM E because of the presence of *Megacricetodon lappi* (Fig. 3). It is therefore similar in age to Ebershausen and Mohrenhausen (Boon 1991) in the western part of the Bavarian Molasse Basin and could be correlated to the base of the Middle Series. In the Swiss part of the Molasse Basin, the Furth locality shows faunal characteristics similar to Frohberg and Aspitobel (Bolliger 1992, 1997; Kälin 1997; Kälin and Kempf 2002).

Localities between Brock horizon and main bentonite layer

Within our studied section we have no fossil localities belonging to OSM E' or F. To date, OSM E' is documented in one locality only (Derching 1b, Augsburg area), found in a sandy unit 2 m below the Brock horizon (Böhme et al. 2002). All localities belonging to OSM F are found between the Brock horizon and the main bentonite layer, both in the Landshut (e.g., Sallmannsberg) and the Augsburg area (e.g., Laimering 3) (Heissig 1997).

^{40}Ar/^{39}Ar chronology

Samples

The Miocene main bentonite in eastern Bavaria has been sampled in a commercially exploited quarry at Hachelstuhl, about 5 km south of Landshut. At this location, the bentonite reveals a trisection typical for most bentonites in the Mainburg–Landshut area. Its central part, a hard bluish-grey, granular to fibrous layer divides the bentonite into a high-quality lower clay and an upper clay of lower montmorillonite content (Ulbig 1994). This hard layer represents the least altered part of the former tuff horizon and contains up to 20% of residual glass fragments.

Similar to the age of the Bavarian main bentonite, and also exposed in the eastern Bavarian Molasse, is the so-called ''Brock horizon''. This central horizon consists of isolated boulders or layers of Upper Jurassic carbonate rocks, which are considered as distal ejecta of the Ries impact at Nördlingen. While radioisotopic ages are ambiguous with respect to the age relationship between the main bentonite and Ries event (Storzer and Gentner 1970), field evidence indicates that Ries ejecta are stratigraphically older (e.g., Unger et al. 1990) and about 30 m below the bentonite (Heissig 1989). For this reason we also analyzed Ries suevite, an impact melt derived from the Phanerozoic basement, as an external control for the bentonite data. The sample was collected at the Öttingen quarry and has kindly been provided by P. Horn (Munich).

Analytical details

The glass-rich central horizon at Hachelstuhl bentonite was previously sampled for chemical analyses by Ulbig (1994; sample Ha-2a). To avoid destroying the fragile glass particles, the rock was treated by thermal disintegration by repeatedly freezing at –25°C and defrosting until the rock disintegrated into smaller parts, which were subsequently dispersed ultrasonically in water and sieved. The grain size fraction (63 μm was treated ultrasonically and the floating clay fraction was repeatedly decanted. In this way, all clay minerals could be effectively removed from the glass particle surfaces.

To obtain clean glass fragments for ^{40}Ar/^{39}Ar dating, associated mineral grains were largely sorted out by Franz magnetic separation and then sieved at different mesh sizes. The maximum-size fraction (125–150 μm) was mildly leached for 5 min in cold 0.2 N hydrofluoric acid in an ultrasonic bath, to remove possible clay-intergrowth and hydrated surfaces, and then ultrasonically treated in deionised water. Clean, fresh and translucent glass shards were then hand-picked under a binocular microscope. Shards showing alteration features, such as yellowish-milky surfaces, clay-intergrowth, mineral inclusions, and gas bubbles, were excluded. The hand-picked glass fraction included 23 mg of overall translucent, elongated, high-porosity glass shards of rhyolitic composition (Ulbig 1999), with shapes characteristic for Plinian-type eruptions.

The tuff and Ries suevite glasses were wrapped in aluminum foil and loaded in 6 mm ID quartz vials. Together with the Fish Canyon Tuff (FCT) sanidine (assumed age 28.02 Ma) and Drachenfels DRA1 (assumed age 25.26 Ma) monitor standards, the samples were irradiated for 1 h with fast neutrons in the Cd-lined RODEO facility of the EU/Petten HFR Reactor (The Netherlands). Argon isotope analysis was carried out at the Department of Isotope Geochemistry, Vrije

Universiteit Amsterdam (The Netherlands), using a MAP 215-50 noble gas mass spectrometer. Eleven and 15 total fusion replicate analyses were carried out for the Hachelstuhl and Ries samples, respectively. The replicate experiments for Ries suevite were conducted in a single session, while those for Hachelstuhl glasses were performed in two sessions. Instrumental mass fractionation was corrected for by repeated analysis of $^{40}Ar/^{38}Ar$ reference gas and $^{40}Ar/^{36}Ar$ air pipette aliquots. Data processing included corrections for blank contribution, mass interferences, regression of mass intensities and mass fractionation using ArAr Calc software (Koppers 2002). Analytical errors refer to 1σ confidence level. Details on the data evaluation and processing can be found in Kuiper et al. (2004).

Results

$^{40}Ar/^{39}Ar$ ages were calculated using the decay constants of Steiger and Jäger (1977), assuming an age of 28.02 Ma for the FCT monitor standard according to the Renne et al. (1998) convention. The data are listed in Tables 2 and 3. Plateau ages in Table 2 refer to weighted means over all accepted total-fusion data. One Ries data and two Hachelstuhl data were considered as outliers and have, therefore, been excluded from the age calculations (Table 2).

Table 2 $^{40}Ar/^{39}Ar$ plateau ages and $^{39}Ar/^{37}Ar$ derived K/Ca ratios of rhyolitic glasses from Hachelstuhl bentonite and suevite impact glasses from Öttingen (Ries)

	Plateau age (Ma)	±2σ	K/Ca	±2σ
Hachelstuhl				
Ha-2a-1[a]	15.21	±0.10	5.079	±0.625
Ha-2a-2[a]	14.91	±0.11	5.179	±0.293
Ha-2a-3	14.80	±0.09	4.890	±0.563
Ha-2a-4	14.79	±0.22	3.305	±0.456
Ha-2a-5	14.79	±0.18	5.172	±0.325
Ha-2a-6	14.74	±0.25	2.915	±0.432
Ha-2a-7	14.71	±0.13	3.692	±0.470
Ha-2a-8	14.66	±0.11	4.686	±0.626
Ha-2a-9	14.59	±0.11	5.389	±0.352
Ha-2a-10	14.58	±0.22	3.239	±0.487
Ha-2a-11	14.58	±0.10	5.370	±0.384
Ries				
Ries-1[a]	17.44	±0.26	1.214	±0.064
Ries-2	15.03	±0.21	1.163	±0.060
Ries-3	15.01	±0.12	1.165	±0.059
Ries-4	14.99	±0.19	1.163	±0.061
Ries-5	14.98	±0.12	1.180	±0.062
Ries-6	14.95	±0.32	1.175	±0.062
Ries-7	14.95	±0.17	1.171	±0.061
Ries-8	14.87	±0.22	1.176	±0.061
Ries-9	14.87	±0.13	1.165	±0.060
Ries-10	14.86	±0.14	1.174	±0.061
Ries-11	14.86	±0.15	1.153	±0.059
Ries-12	14.84	±0.14	1.197	±0.062
Ries-13	14.83	±0.13	1.156	±0.059
Ries-14	14.82	±0.16	1.167	±0.060
Ries-15	14.79	±0.10	1.162	±0.059

[a] Rejected

Table 3 Summary of $^{40}Ar/^{39}Ar$ plateau and isochron ages of rhyolitic glasses from Hachelstuhl bentonite and suevite impact glasses from Öttingen (Ries)

	Hachelstuhl	*n*	Ries	*n*
Weighted plateau (Ma)	14.68 ± 0.11	9	14.89 ± 0.10	14
MSWD	2.33		1.26	
$^{39}Ar_K$ used in plateau calc.	71%		96.3%	
Total fusion (Ma)	14.82 ± 0.10	11	14.99 ± 0.10	15
Normal isochrone (Ma)	14.56 ± 0.19	9	14.88 ± 0.11	14
Non-radiogenic $^{40}Ar/^{36}Ar$ intercept	313.8 ± 23.5		273.2 ± 85.1	
MSWD	1.73		2.66	
Inverse isochrone (Ma)	14.54 ± 0.19	9	14.84 ± 0.11	14
Non-radiogenic $^{40}Ar/^{36}Ar$ intercept	317.6 ± 24.4		360.8 ± 67.1	
MSWD	1.75		0.92	
Suggested age (Ma)	14.55 ± 0.19		14.88 ± 0.11	

n Number of analyses

Eleven total fusion experiments were performed for Hachelstuhl tuff glasses. The K/Ca ratios (Table 2), which were derived from $^{39}Ar/^{37}Ar$, are consistent with the degree of variation in the chemical composition of the glasses, as observed by electron microprobe analysis, and are not correlated with age (not shown). This indicates that possible preferential loss of K during late alteration did not affect the glasses and, hence, the $^{40}Ar/^{39}Ar$ ages. Nine out of the eleven fusion data were used for the age calculation, yielding a weighted plateau age of 14.68 ± 0.11 Ma. Within error, this age is identical to the normal isochron (14.56 ± 0.19 Ma) and inverse isochron ages (14.54 ± 0.19 Ma). Plateau ages of individual total fusion experiments and the runs chosen to calculate the weighted plateau ages are listed in Table 2 and in Fig. 4.

There is an apparent 100 ka offset between plateau and isochron ages, which may be due to some excess argon present in some of the Hachelstuhl samples. Hence, the three lowest plateau ages would best represent the ''true'' age. The isochron excess argon intercept supports this interpretation and the lower isochron age is consistent with the ages obtained for the three youngest steps. Based on these arguments we estimate an age of 14.55 ± 0.19 Ma for the Hachelstuhl tuff. This age compares well with fission track data of main bentonite glasses from Mainburg and Unter-Haarland/Malgersdorf, yielding ages of 14.6 ± 0.8 and 14.4 ± 0.8 Ma, respectively (Storzer and Gentner

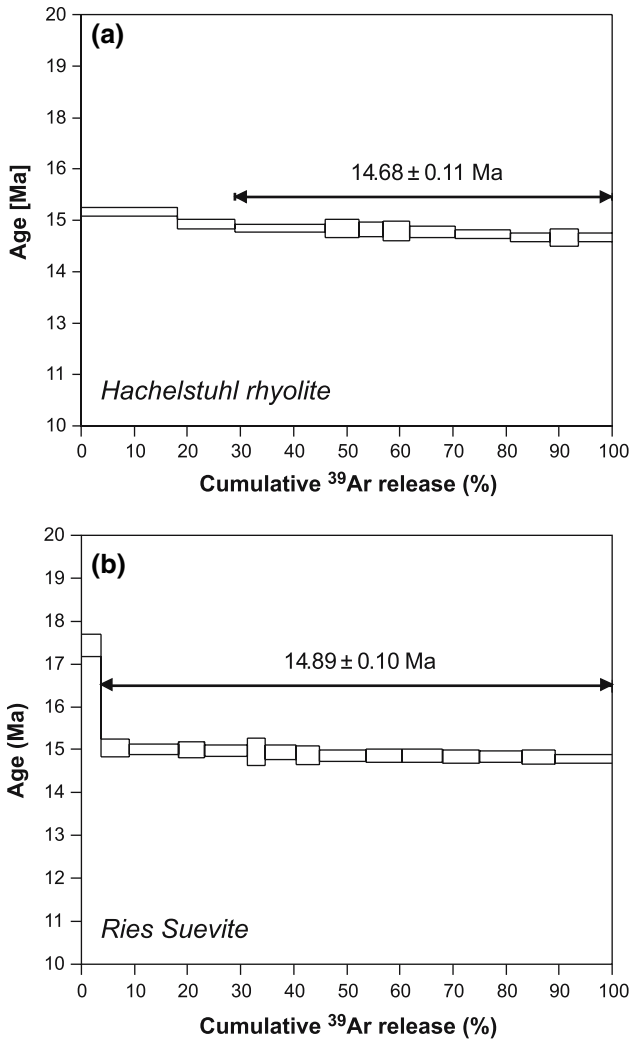

Fig. 4 Weighted mean plateau ages of individual total fusion experiments and runs for Hachelstuhl (**a**) and Ries glasses (**b**). Plateau steps and their 1σ error are shown. (Total procedure blanks ranged from 1.2×10^{-3} to 3.8×10^{-3} for mass 36, 1.0×10^{-3} to 3.2×10^{-3} V for mass 37, 0.2×10^{-4} to 13×10^{-4} V for mass 38, 0.6×10^{-4} to 3.1×10^{-4} V for mass 39, and 2.3×10^{-2} to 4.8×10^{-2} V for mass 40, based on a system sensitivity of 1.8. 10^{-17} mol/V)

1970). We are not aware of any other age determinations for the main bentonite.

For the Ries suevite glass we obtain a weighted plateau age (14 out of 15 total fusion experiments) of 14.89 ± 0.10 Ma, which is identical to the normal (14.88 ± 0.11 Ma) and inverse isochron ages (14.84 ± 0.11 Ma). Again, K/Ca ratios reflect the chemical composition of the suevite and do not correlate with age (Table 2). Plateau ages of individual total fusion experiments and the runs chosen to calculate the weighted plateau ages are listed in Table 2 and shown in Fig. 4. Except for one, all analyses yield very consistent results. Based on these results and the consistency of plateau and isochron ages, we suggest an age of 14.88 ± 0.11 Ma for the Ries impact glasses. This age is identical to the mean (14.87 ± 0.36 Ma) of 51 published K–Ar, $^{40}Ar/^{39}Ar$, and fission track ages compiled by Storzer et al. (1995), but up to 0.5 Ma older than the more recent data on moldavites and Ries glasses (Schwarz and Lippolt 2002; Laurenzi et al. 2003; Buchner et al. 2003).

Magnetostratigraphy

Samples and methods

The nine sections sampled for paleomagnetic analysis coincide, in many cases, with important vertebrate fossil localities. Our aim was to sample at a resolution of 5–10 cm; however, due to variable lithologies the samples are unevenly spaced throughout the sections. All samples were hand-cored in—often unconsolidated—fine sands and silts or in clays and oriented using a standard compass. Since the samples were fragile, they were subsequently pushed into plastic cylinders. The initial magnetic susceptibility of the samples was measured on a Kappa bridge KLY-2. The characteristic remanent magnetization (ChRM) was determined by both thermal (TH) and alternating field (AF) demagnetization using in a laboratory-built shielded furnace and a single axis AF-demagnetizer (ambient field (5 nT), respectively. During thermal demagnetization, the plastic cylinder of each sample was carefully removed and replaced by a thermally demagnetized (at 700°C) ceramic cylinder. The samples were thermally demagnetized using incremental heating steps of 20, 40 and 50°C. AF demagnetization was carried out in small steps of 5 mT up to 30 mT, followed by steps of 10 mT up to a maximum field of 200 mT. The natural remanent magnetization (NRM) was measured on a vertically oriented 2G Enterprises DC SQUID cryogenic magnetometer (noise level 10–7 A/m) in a magnetically shielded room at the Niederlippach paleomagnetic laboratory of Ludwig-Maximilians-University Munich, Germany. Demagnetization results were plotted on orthogonal vector diagrams (Zijderveld 1967) and ChRM directions were calculated using principle component analysis (PCA, Kirschvink 1980).

Results

The TH and AF demagnetization diagrams of the approximately 450 measured samples are of variable quality (Fig. 5). NRM intensities are low, varying

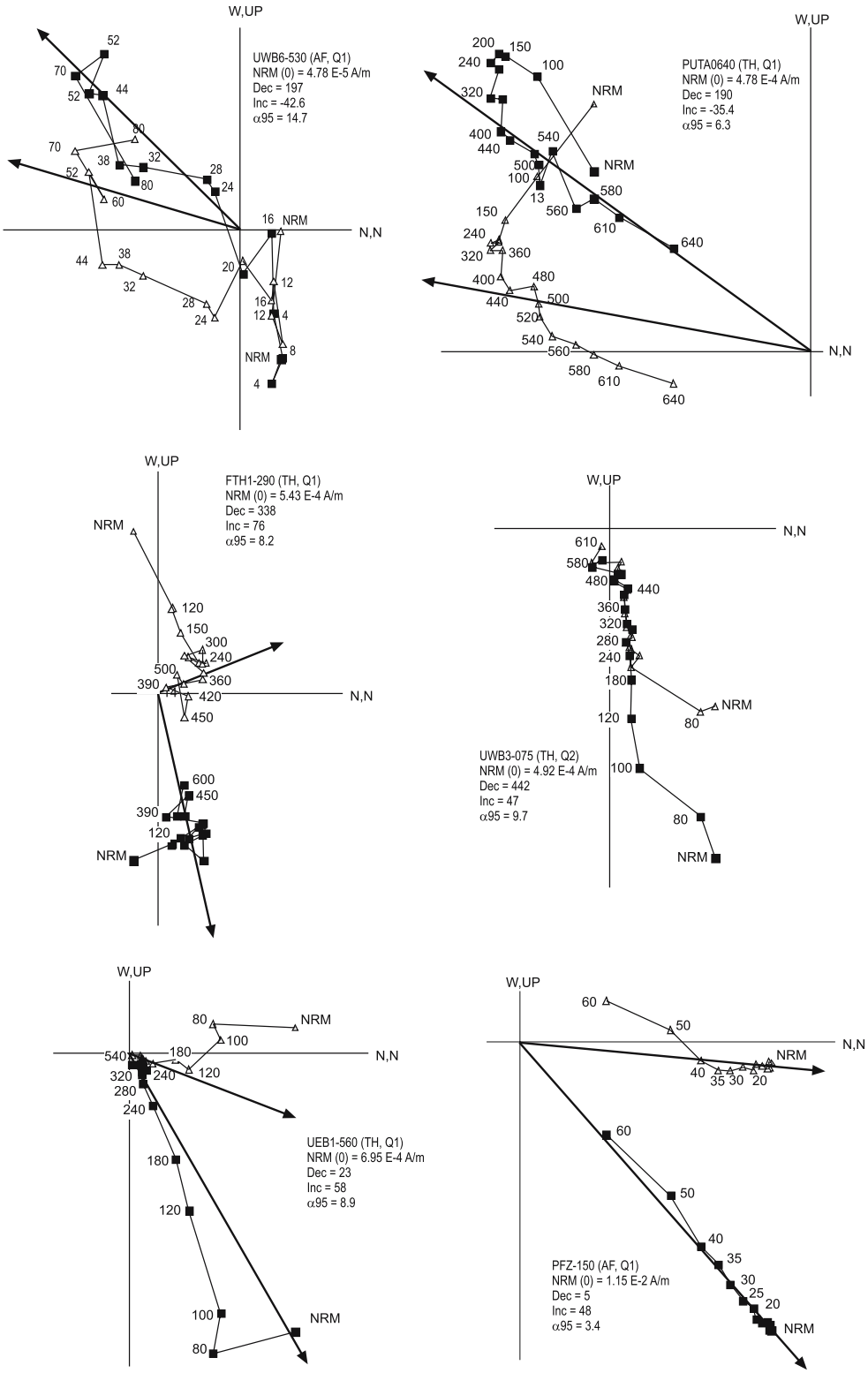

Fig. 5 Thermal (TH) and alternating field (AF) demagnetization diagrams for selected samples of the studied eastern Bavarian sections. *Black rectangles* (*white triangles*) denotes the projection on the vertical (horizontal) scale. Values along demagnetization trajectories indicate temperature and applied field steps in °C and mT, respectively. *Q1* and *Q2* denote quality 1 and 2 type of demagnetization, respectively (see text for details)

between 0.05 and 100 mA/m (average 0.8 mA/m) with only a few values reaching up to 2,450 mA/m for red paleosols in the Puttenhausen section. TH and AF demagnetization show that most of the samples carry three components (Fig. 5). The first component shows a random oriented, viscous direction, which is removed at temperatures of 100°C and at fields of 2 mT. A second component is removed between 100 and 200°C and at 15 mT, and is interpreted as the present-day field overprint. In Pfaffenzell and Puttenhausen

sections, a low temperature component is removed at 360°C.

The third component is removed at higher temperatures, ranging between 480 and 580°C suggesting that the magnetic signal is carried by magnetite. Higher unblocking temperatures between 600 and 680°C are found for few samples from Puttenhausen, Pfaffenzell and Unterempfenbach sections and are usually associated with paleosol horizons, suggesting the presence of (fine-grained) hematite. As for the AF demagnetized samples, the magnetic remanence is fully demagnetized between 60 and 80 mT. Although a few samples are also demagnetized at fields up to 120 mT, a significant progressive increase in intensity is often observed when demagnetizing at fields higher than 80 mT.

Because of the variable quality of the Zijderveld diagrams and different temperature and AF ranges of demagnetization we used the following criteria to determine the ChRM direction in the third component: (1) reliable ChRM direction must be observed in the temperature range 240/360–480°C or higher and the AF field range 20–50 mT or higher, and (2) within these windows at least four stable end points must be used for PCA calculation of the ChRM direction. Based on these criteria, three ChRM demagnetization qualities are distinguished. (1) About 37% of both TH and AF demagnetized samples belong to the quality 1 type of demagnetization, characterized by a clear and stable demagnetization showing a more or less linear decay towards the origin. Except for the Pfaffenzell section, dual polarities are recorded in all sections. (2) Samples with quality 2 type of demagnetization show fair demagnetization behavior, however, no clear decay to the origin can be observed. Rather, the ChRM end-points show a cluster in either the normal or reversed quadrants. About 21% of thermally and 16% of the AF demagnetized samples belong to this quality group. (3) The majority of the demagnetized samples, which comprise 54% thermal and 57% AF treated samples, are assigned quality 3 type of demagnetization. The Zijderveld diagrams of these samples do not show any clear demagnetization path nor do they meet the two criteria; they are therefore non-interpretable.

Since the sections are more or less in the vicinity of each other, we have calculated the average direction of for all quality 1 samples with a MAD smaller than 15 (Fig. 5). The average declination/inclination is 358/56 for the normal samples (n = 83) and 183/–44 for the reverse samples (n = 27). Notably, the number of reverse samples is limited and the scatter is rather large (α_{95} = 10.8). In addition, the inclination of the reversed samples is shallower by 10° compared to the normal values, which could be explained by a possible secondary normal overprint making it impossible to completely isolate the primary ChRM component. Mean directions of the ChRM should therefore be treated with caution when interpreted in terms of tectonic rotations.

Reliability of the polarity signal

For each section, all quality 1 declination and inclination results have been plotted in stratigraphic order (Figs. 6, 7). Since the studied sections are horizontally bedded, no bedding-tilt correction could be applied and therefore it is impossible to distinguish primary from secondary components. Most of the magnetostratigraphic records, however, show dual polarities and/or similar polarity directions were obtained for AF as well as thermally demagnetized samples. Therefore, we consider that most of the studied records are reliable. An exception is the Puttenhausen section, which reveals several polarity reversals but most polarity directions of the AF demagnetized samples do not agree with the directions obtained for the thermal samples. Moreover, the quality 1 AF demagnetized samples are, except for one sample, all normal. Based on the unblocking temperatures (~630°) we assume that the ChRM of the Puttenhausen samples is carried by fine-grained hematite having a low temperature normal overprint, which cannot be resolved using the AF demagnetization method. Hence, the polarity record of Puttenhausen is based on ChRM directions from thermally demagnetized samples only.

Magnetostratigraphic calibration

The polarity records of the studied sections comprise none or only a few reversal levels and are insufficient for a direct and unambiguous magnetostratigraphic correlation to the ATNTS04 (Lourens et al. 2004). Hence, to establish a chronostratigraphic framework for the eastern Bavarian Upper Freshwater Molasse, the magnetostratigraphic results are combined with biostratigraphic and lithostratigraphic correlations established between sections and with $^{40}Ar/^{39}Ar$ ages (Fig. 8).

The youngest interval: Sand-Mergel-Decke (SMD) and main bentonite horizon

The youngest sections belonging to the main bentonite layer and the SMD include Pfaffenzell, Bruckberg and the uppermost part of Unterwattenbach. The main

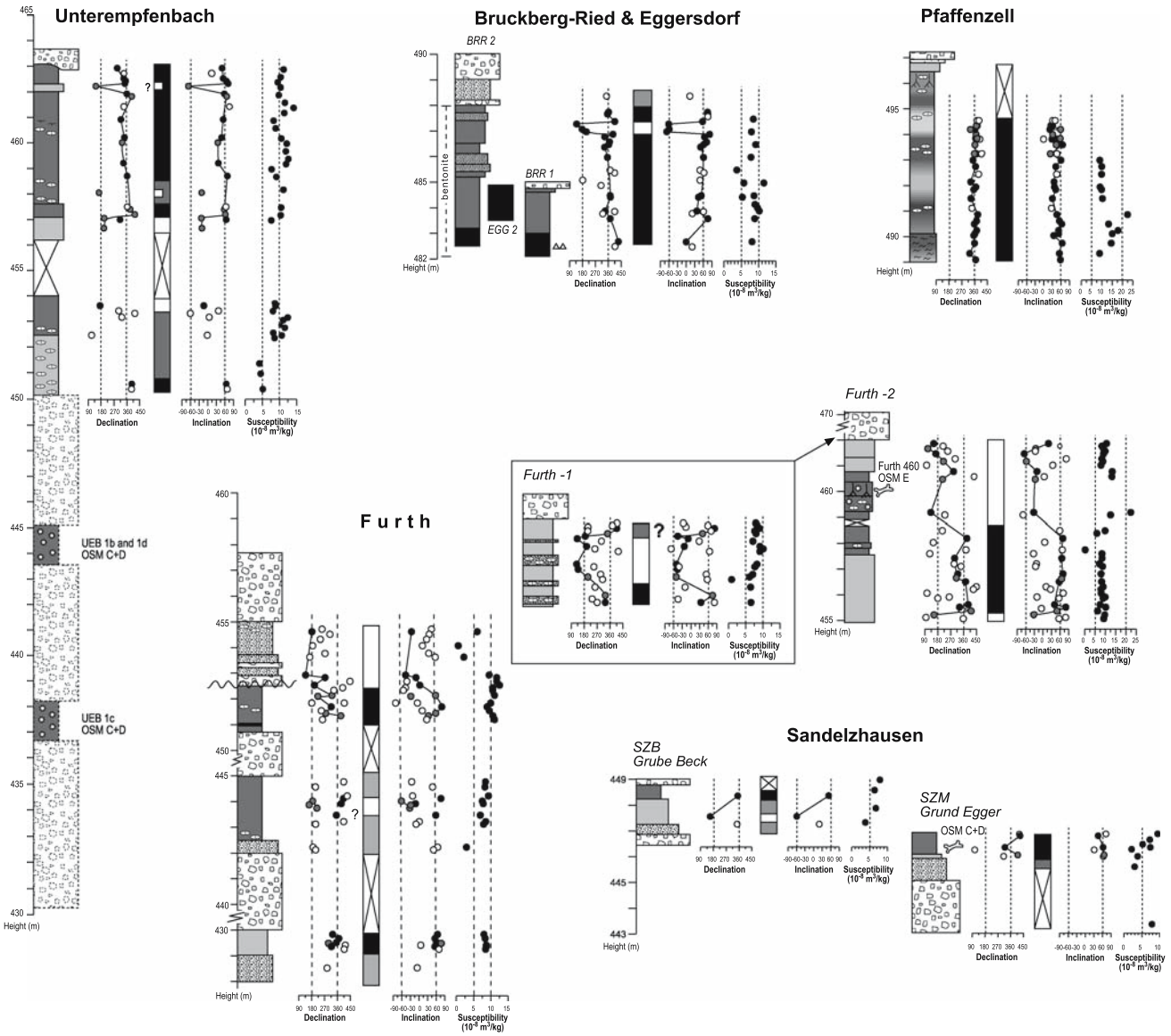

Fig. 6 Lithology columns, paleomagnetic results and polarity columns for the eastern Bavarian Molasse sections. The *black* and *grey dots* in the declination and inclination records represent quality 1 ChRM directions for alternating field (AF) and thermal (TH) demagnetized samples, respectively. The *white dots* represent quality 2 type of demagnetizations for both AF and TH treated samples. In the polarity columns, *black* (*white*) *zones* indicate normal (reversed) polarity and *grey shaded zones* uncertain polarity. The stratigraphic position of Furth 1 with respect to Furth 2 section is indicated. For explanation of lithology columns, see legend in Fig. 2

bentonite, sampled at Hachelstuhl, is found in all (or in the vicinity of) sections. Using the all the time-stratigraphic constraints, we correlate the short reversed polarity in Bruckberg-Ried to C5ACr, the normal polarity of Pfaffenzell to C5ADn and the reversed polarity R1 in Unterwattenbach to C5ADr. These correlations imply that the Hachelstuhl bentonite occurs in the lower part of chron C5ADn, which closely corresponds to our $^{40}Ar/^{39}Ar$ estimated age of 14.55 (±0.19) Ma.

The middle interval: the Brock horizon

The sections in the middle part belong to the upper part of the NV (Hangender Teil) and the Zwischenmergel (ZM) and include Unterempfenbach, Kreut, Furth 1 and 2 and the upper part of Unterwattenbach (R1 to R2). We correlate the long upper normal polarity of Unterempfenbach to C5Bn.1n and the lowermost to C5Bn.2n. Since Furth 1 represents a channel fill postdating the deposits of Furth 2 section,

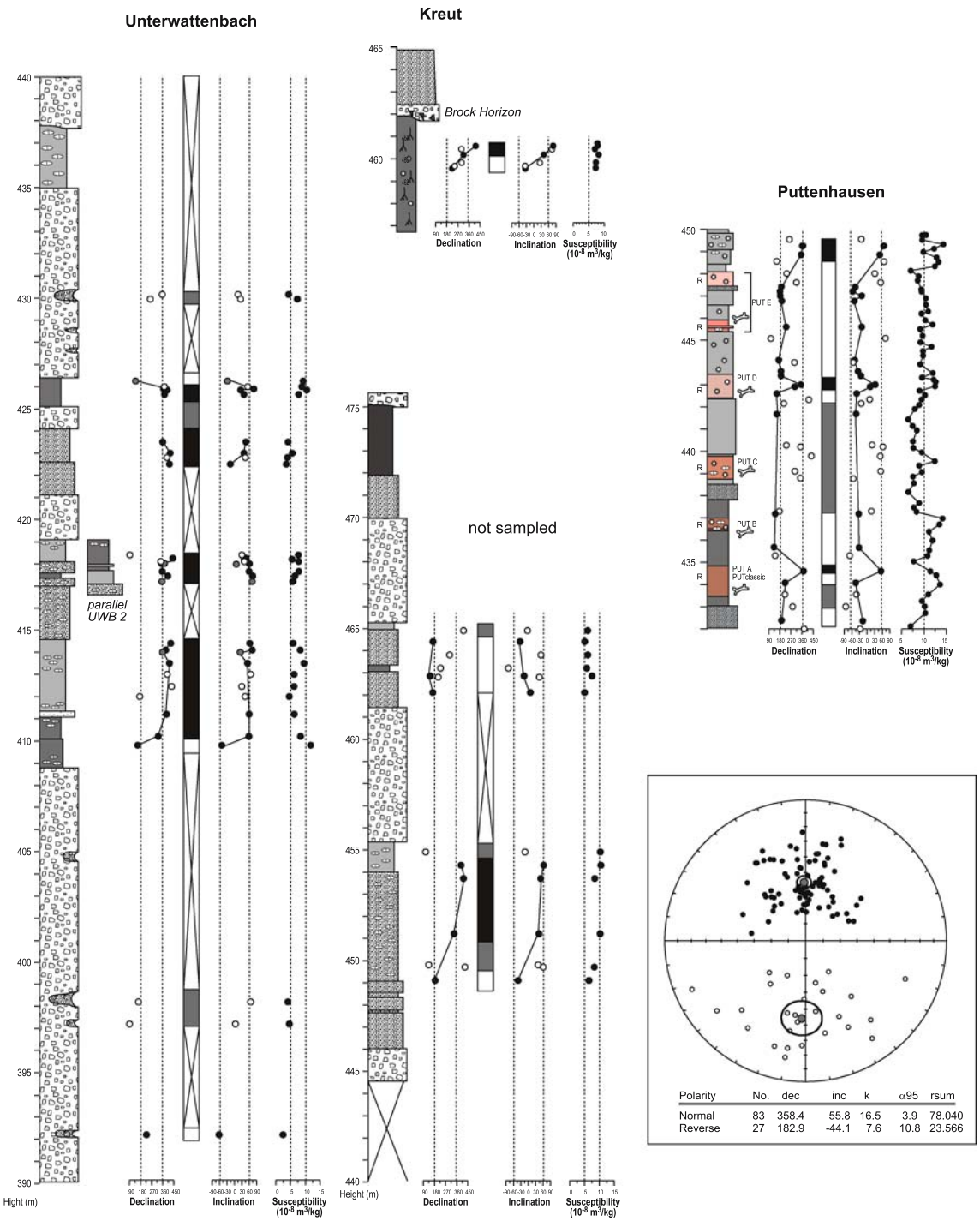

Fig. 7 Lithology columns, paleomagnetic results and polarity columns for the eastern Bavarian Molasse sections (see caption to Fig. 6). Inset: equal area projection of quality 1 ChRM directions (with MAD values <15) for all sections. The 95% confidence ellipse for the normal and reverse directions is indicated. Statistical information includes number of samples (*No.*), declination (*Dec.*), inclination (*Inc.*), Fisher's parameter (k) and radius of the 95% confidence cone ($\alpha 95$). For explanation of lithology columns, see legend in Fig. 2

the reversed polarity in this section is therefore correlated to chron C5ADr. The upper reversed polarity of Furth 2 correlates to CBn.1r and R2 in Unterwattenbach to the top of C5Br. This implies that the Brock horizon, which is only found in Kreut section in a gravel interval (incising the underlying ZM) where

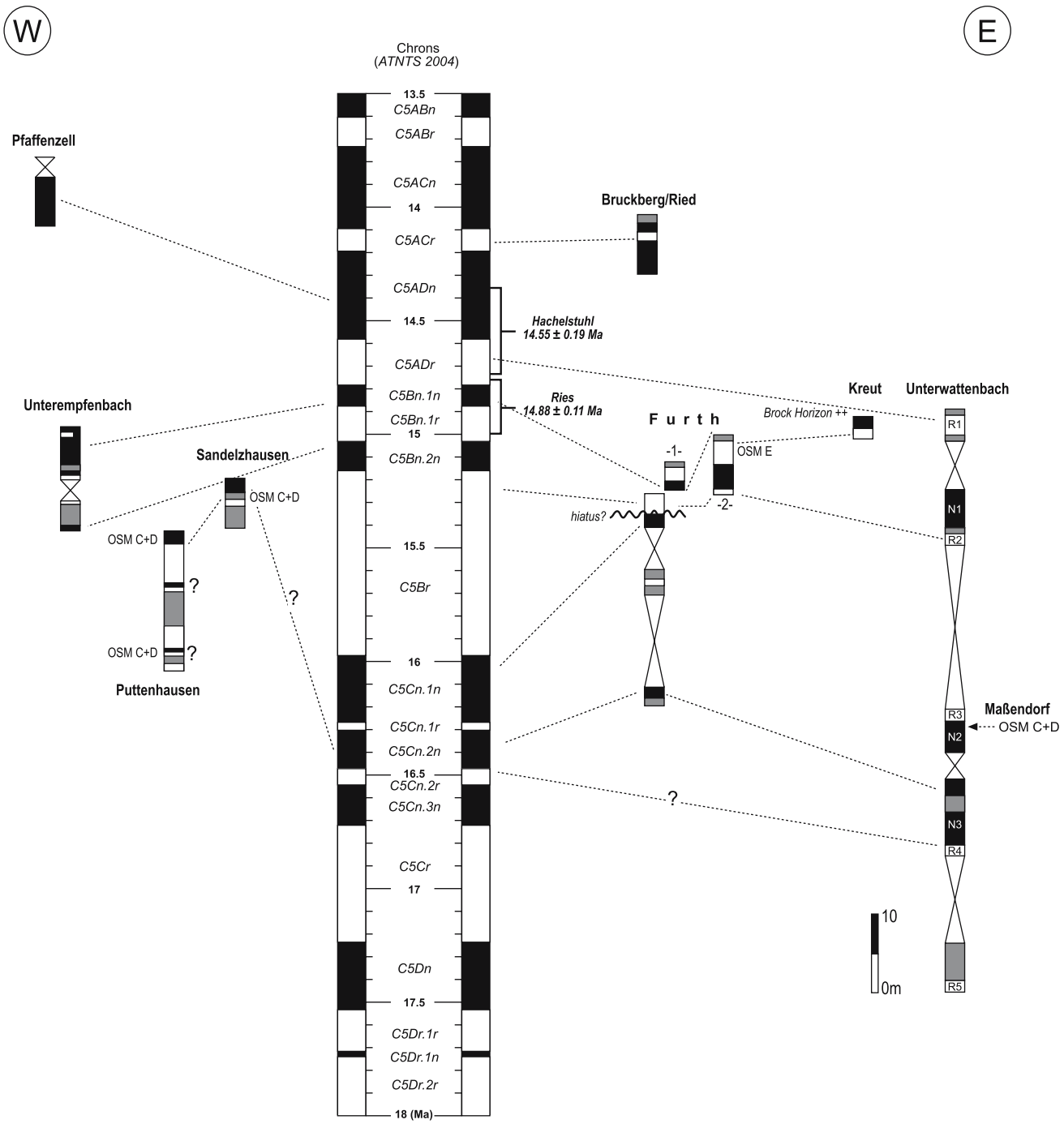

Fig. 8 Calibration of eastern Bavarian magnetostratigraphic records to the Astronomical Tuned Neogene Time Scale (ATNTS04) of Lourens et al. 2004. The $^{40}Ar/^{39}Ar$ ages of the Ries and Hachelstuhl glasses are displayed with their 1σ analytical error

no polarity direction could be obtained, either occurs in chron C5Bn.1n or in C5ADr. Past paelomagnetic studies on Ries suevites have indicated a reversed polarity signal (Pohl 1965; Petersen et al. 1965) hence suggesting that the Brock horizon falls within chron C5ADr, yielding an age between 14.581 and 14.784 Ma (average 14.68 ± 0.1 Ma). This age more or less coincides within error to our estimated $^{40}Ar/^{39}Ar$ age of 14.88 ± 0.11 Ma for the Ries suevites from Öttingen.

The oldest interval: OSM C biozonation

The sections in this interval belong to the lower part of the NV and Süßwasser Kalk (SK) and include Furth, Sandelzhausen, Puttenhausen and the middle and

lower part of Unterwattenbach (R3 to R5). The unclear magnetic polarity records hamper a straightforward correlation to the ATNTS04. Nevertheless, using the biostratigraphy (OSM C + D fauna) of the sections, the uppermost normal level in the long Furth section is correlated to C5Cn.1n. The small-mammal fauna of Sandelzhausen and uppermost part of Puttenhausen show similar characteristics and all coincide with a normal polarity interval, which possibly correlates to C5Cn.2n. The reversed zone R4 in Unterwattenbach correlates to C5Cn.2r. The unclear polarity in the lower part of Puttenhausen prohibits any reliable correlation to the ATNTS04.

Discussion

Pre-Riesian hiatus

It must be noted that our magnetostratigraphic correlations to the ATNTS04 represent best-fit correlations and could be interpreted differently. The correlations established for the youngest and middle intervals seem rather robust and are supported by lithostratigraphic field observations as well as $^{40}Ar/^{39}Ar$ ages for the main-bentonite sampled at Hachelstuhl.

The most obvious feature of this correlation, however, is the absence of the long reversed interval of C5Br in the sections of eastern Bavaria. This absence could be explained by the presence of a sedimentary gap, the so-called pre-Riesian hiatus. Indications of a hiatus have been found in the sedimentary record at the northern margin of the Bavarian part of the Molasse Basin with up to 150 m deep erosional channels (Birzer 1969) and as a turnover in the mammal record throughout the basin (Böhme et al. 2002). This turnover is contemporaneous with a stratigraphic gap between biostratigraphic units OSM C + D and OSM E (Fig. 3). Similarly, several sedimentary gaps, which may be associated with the hiatus, are present in sections in the Swiss Molasse (Kempf et al. 1997). In the eastern Alpine area several hiatuses have been recognized in the Austrian part of the Molasse Basin (Rögl et al. 2002) and in other Austrian Neogene basins (Rögl et al. 2006) attributed to the Styrian phase of Stille (1924). Nevertheless, since the magnetostratigraphic records of our sections in this time-interval are not well-constrained—especially the Puttenhausen section, which we aim to re-sample and extend upward in the near future—we do not exclude that inconsistencies may be present in the calibration to the ATNTS04.

Biostratigraphic implications

Our best-fit magnetostratigraphic correlation allows calibration of the micro-mammal fauna's of the eastern Bavarian Molasse with the ATNTS04 enabling a comparison with the faunal records from the Swiss Molasse Basin. We refrain from using MN ''zones'' for comparisons because these ''zones'' are defined by evolutionary levels, faunal distribution patterns and presence of important taxa (Bolliger 1997; Heissig 1997) of which the latter two may vary geographically due to ecological differences and migration events. Therefore, no reliable comparisons can be made especially when aiming at understanding detailed faunal changes in a short time interval, such as the case in this study. Hence, only the local OSM zones are used for comparison.

The OSM F faunal unit in eastern Bavaria corresponds to reference level Rümikon in the Swiss Molasse Basin, which correlate to C5ADn (Kälin and Kempf 2002). This agrees with our magnetostratigraphic calibration of the sections between the Brock horizon and the main bentonite layer. The fauna of OSM E', stratigraphically below the Brock horizon, is similar to the Chatzloch fauna which is correlated to C5ADr (Kälin and Kempf 2002) and also agrees with our calibration of the Furth 1 section.

The micro-mammal fauna unit OSM E, found in our studied Furth 2 section, has similar faunal characteristics as Frohberg locality in the Swiss Molasse (Bolliger 1992). The magnetostratigraphic calibration to chron C5Bn.1r agrees well with Frohberg, which correlates to the same chron (Kempf et al. 1997; Schlunegger et al. 1996). Based on the evolutionary stage of *Megacricetedon* aff. *bavaricus*, the younger part of faunal unit OSM C + D defined in localities Sandelzhausen and upper part of Puttenhausen (PUT E) is very similar to the Swiss fauna's from Tobelholz and Vermes 2 (Reichenbacher et al. 2005). However, the relationship of Toblholz and Vermes 2 to the Tobel Hombrechtikon fauna, which is magnetostratigraphically correlated to chron C5Bn.2 (Kälin and Kempf 2002), is unclear because of the lack *M.* aff *bavaricus* (Kälin 1997). Therefore, the magnetostratigraphic calibration of the Swiss localities is not reliable.

The older OSM C + D fauna is found in the Puttenhausen section (PUT classic), and corresponds to the Swiss reference fauna of Vermes 1, also defined in the magnetostratigraphic calibrated locality of Martinsbrünneli (Kempf et al. 1997; Heissig 1997). Martinsbrünneli and the fauna of Hüllistein are situated below the Hüllistein marker bed, which coincides with the boundary of C5Br/C5Cn.1n (Kempf et al. 1997).

Based on the evolutionary stage of *M*. aff. *bavaricus*, however, Hüllistein is clearly older than Sandelzhausen and all Puttenhausen levels (Fig. 3). At this moment we correlate the younger faunas of OSM C + D to C5Cn.1r/C5Cn.1n yielding an age discrepancy of about 500 ka with respect to the Swiss calibration. This large discrepancy can be related to the poor quality of the Puttenhausen polarity record and hence an incorrect calibration to the ATNTS04.

Comparison with $^{40}Ar/^{39}Ar$ ages

The magnetostratigraphic calibrated age for the Hachelstuhl bentonite to the lower part of chron C5ADn (~14.5 Ma) of the ATNTS04 closely coincides with our $^{40}Ar/^{39}Ar$ estimated age of 14.55 (±0.19) Ma. So far, the main bentonite horizon in eastern Bavaria has only been dated by fission track analysis. Storzer and Gentner (1970) sampled the main bentonite at Mainburg and Unter-Haarland and found fission track ages of 14.6 ± 0.8 and 14.4 ± 0.8 Ma, respectively. These data are very similar to our estimated age of 14.55 ± 0.19 Ma. Since fission track and $^{40}Ar/^{39}Ar$ dating are two independent radiometric dating methods, which not only differ in analytical approach but also in decay systematics and constants, the consistency between both data sets suggests that the Hachelstuhl bentonite age is very robust.

Although within error, the estimated $^{40}Ar/^{39}Ar$ age for the Ries glass is about 200 kyr older than the magnetostratigraphic calibrated ATNTS04 age of ~14.68 ± 0.10 Ma for the Brock horizon. However, the magnetostratigraphic calibration of the Ries impact supports earlier calibration efforts established in the Swiss Molasse (Schlunegger et al. 1996). Similar to the main bentonite, our ATNTS04 age for the Ries event is identical to fission track ages: Storzer et al. (1995) analyzed 15 Ries glasses, yielding a mean age of 14.68 ± 0.25 Ma. Hence, the magnetostratigraphic calibrated age for the Brock horizon seems convincing.

Our $^{40}Ar/^{39}Ar$ age estimate of 14.88 ± 0.11 Ma compares well with mean argon ages determined by Storzer et al. (1995). They evaluated 15 fission track ages (mean 14.68 ± 0.25 Ma) and 12 argon ages (mean 15.14 ± 0.51 Ma) of Ries suevite and 7 fission track ages (mean 14.82 ± 0.18 Ma) and 17 argon ages (mean 14.82 ± 0.32 Ma) of moldavites. All weighted means for both the different impact glasses and methods are, within error, identical to our results.

In contrast, recently published $^{40}Ar/^{39}Ar$ ages of Ries ejecta are up to 550 ka younger. Schwarz and Lippolt (2002) report plateau ages of 14.50 ± 0.16 and 14.38 ± 0.26 Ma for tectites from Bohemia and Lutetia, respectively. Laurenzi et al. (2003) obtained an average laser total fusion age of 14.34 ± 0.08 Ma for Bohemian and Moravian moldavites while Buchner et al. (2003) found a $^{40}Ar/^{39}Ar$ laser total fusion value of 14.32 ± 0.28 Ma for a Ries suevite. The large age difference may partly be explained by the different monitor standards and/or their assumed ages used in these studies. For example, Laurenzi et al. (2003) use an age of 27.95 Ma for the FCT standard while Schwarz and Lippolt (2002) use a HD-B1 bt standard that is not cross-calibrated to the Fish Canyon standard (Laurenzi et al. 2003). Similarly, Buchner et al. (2003) used a third standard (TCs-1) with an age of 27.92 Ma.

Buchner et al. (2003), however, explain that the published suevite ages older than 14.3 Ma could be due to the presence of relict minerals in the Ries glass, derived from the Paleozoic basement. Although this explanation could account for the 200 kyr offset between our $^{40}Ar/^{39}Ar$ and ATNTS04 ages, several observations argue against it. Relict minerals have, to our knowledge, not been reported from moldavites and their absence is convincingly demonstrated in the extensive data set of Laurenzi et al. (2003) and Schwarz and Lippolt (2002). Laurenzi et al. (2003) obtained 76 plateau ages from analysis of seven different moldavites, of which the ages varied by 400 ka only. It is therefore highly unlikely that such age uniformity can be obtained with relict minerals. Moreover, the Schwarz and Lippolt step-heating plateaus are very uniform and the high-temperature steps do not indicate the presence of relict minerals.

Finally, moldavites and Ries glasses originated from different source rocks, namely Miocene sedimentary cover and Paleozoic basement, respectively (Graup et al. 1981). In the case of inherited argon, Ries glasses should yield different and characteristic age spectra for the two rock types, which this is not the case (Storzer et al. 1995, see above). We thus conclude that although the different monitor standards could partially account for the inconsistency between the different ages obtained for Ries ejecta, a satisfactory explanation for this inconsistency remains unresolved.

Conclusions

Paleomagnetic analysis was performed using two different demagnetization methods: AF and TH demagnetization. The AF method revealed both normal and reverse polarities but proofs not to be reliable for samples with the primary ChRM carried by fine-grained hematite.

The magnetostratigraphic calibration of the studied sections to the ATNTS04 gives reliable results for the youngest and middle intervals. The three biostratigraphic units OSM E, E' and F are correlated to chrons C5Bn.1r, C5ADn and C5ADn, respectively. This is confirmed by radioisotopic dating of the Brock horizon (14.88 ± 0.11 Ma) and the main bentonite layer (14.55 ± 0.19 Ma).

So far, the results for the older interval (OSM C + D) are ambiguous. A long hiatus (pre-Riesian hiatus) of several hundred thousand years separating OSM C + D from OSM E may be present within chron C5Br. However, we do not exclude that the poor quality of the Puttenhausen polarity record resulted in an incorrect calibration to the ATNTS04.

Acknowledgments We thank Daniel Kälin and Johann Hohenegger for critically reviewing the manuscript. Georg Bauer (Ziegelwerke Leipfinger-Bader, Puttenhausen), Franz Luderfinger (Isarkies GmBH, Unterwattenbach) and Helmut Eichstetter (Eichstetter GmBH, Furth) are thanked for working permissions and technical help in the gravel and clay pits. Albert Ulbig is thanked for providing the glass samples from Hachelstuhl. This project was supported by DFG grant BO 1550/7–1.

References

Bachmann GH, Müller M (1991) The Molasse Basin, Germany: evolution of a classic petroliferous foreland basin. In: Spencer AM (ed) Generation, accumulation, and production of Europe's hydrocarbons. Special publication of the European association of petroleum geoscientists. Eur Assoc Pet Geosci Spec Publ 1. Oxford University Press, Oxford, pp 263–276

Batsche H (1957) Geologische Untersuchungen in der Oberen Süßwassermolasse Ostniederbayerns (Blatt Landau, Eichendorf, Simbach, Arnstorf der Topogr. Karte 1:25,000). Beihefte zum Geologischen Jahrbuch 26:261–307

Birzer F (1969) Molasse und Ries-Schutt im westlichen Teil der südlichen Frankenalb. Geologische Blätter für Nordost-Bayern 19:1–28

Böhme M (1999) Die miozäne Fossil-Lagerstätte Sandelzhausen. 16. Fisch- und Herpetofauna-Erste Ergebnisse. Neues Jahrb Palaontol Geol Abh 214(3):487–495

Böhme M (2003) Miocene climatic optimum: evidence from lower vertebrates of Central Europe. Palaeogeogr Palaeoclimatol Palaeoecol 195(3–4):389–401

Böhme M, Gregor H-J, Heissig K (2002) The Ries- and Steinheim meteorite impacts and their effect on environmental conditions in time and space. In: Buffetaut E, Koerbel C (eds) Geological and biological effects of impact events. Springer, Berlin, pp 215–235

Bolliger T (1992) Kleinsäuger aus der Miozänmolasse der Ostschweiz. Doc nat 75:296

Bolliger T (1997) The current knowledge of the biozonation with small mammals in the upper fresh water molasse in Switzerland, especially the Hörnli-Fan. In: Aguilar JP, Legendre S, Michaux J (eds) Actes du Congres BiochroM'97. Mem Trav EPHE, Inst Montpellier 21, pp 537–546

Boon E (1991) Die Cricetiden und Sciuriden der Oberen Süßwasser-Molasse von Bayerisch-Schwaben und ihre stratigraphische Bedeutung. Ph.D. thesis, Ludwig-Maximillians-University Munich, p 159

Buchner E, Seyfried H, van den Bogaard P (2003) $^{40}Ar/^{39}Ar$ laser probe age determination confirms the Ries impact crater as the source of glass particles in Grupensand sediments (Grimmelfingen formation, North Alpine Foreland Basin). Int J Earth Sci 92:1–6

Dehm R (1955) Die Säugetierfaunen der Oberen Süßwassermolasse und ihre Bedeutung für die Gliederung. Erläuterungen zur Geologischen Übersichtskarte der Süddeutschen Molasse. Bayerisches Geologisches Landesamt, Munich, pp 81–87

Doppler G, Pürner T, Seidel M (2000) Zur Gliederung und Kartierung der bayerischen Vorlandmolasse. Geol Bavarica 105:219–243

Fahlbusch V (1964) Die Cricetiden (Mamm.) der Oberen Süßwassermolasse. Bayer Akad Wiss Math Naturwiss Kl Abh (NF) 118:136

Fahlbusch V (2003) Die miozäne Fossil-Lagerstätte Sandelzhausen—Die Ausgrabungen 1994–2001. Zitteliana A 43:109–122

Fahlbusch V, Wu W (1981) Puttenhausen: Eine neue Kleinsäuger-Fauna aus der oberen Süßwasser-Molasse Niederbayerns. Mitt Bayer Staatssammlung für Paläont historische Geol 21:115–119

Fahlbusch V, Gall H, Schmidt-Kittler N (1972) Die obermiozäne Fossil-Lagerstätte Sandelzhausen. 2. Sediment und Fossilgehalt. N Jb Geol Paläont Mh 1972(6):331–343

Fiest W (1989) Lithostratigraphie und Schwermineralgehalt der Mittleren und Jüngeren Serie der Oberen Süßwassermolasse Bayerns im Übergangsbereich zwischen Ost- und Westmolasse. Geol Bavarica 94:259–279

Graup G, Horn P, Köhler H, Müller-Sohnius D (1981) Source materials for moldavites and bentonites. Naturwissenschaften 68:616–617

Gregor J (1969) Geologische Untersuchungen im Südost-Viertel des Blattes Mainburg 7336 (Niederbayern). Graduate thesis, Ludwig-Maximilians-University Munich, p 59

Heissig K (1989) Neue Ergebnisse zur Statigraphie der Mittleren Serie der Oberen Süßwassermolasse Bayerns. Geol Bavarica 94:239–258

Heissig K (1990) The faunal succession of the Bavarian Molasse reconsidered—correlation of the MN5 and MN6 faunas. In: Lindsay EH, Fahlbusch V, Mein P (eds) European Mammal Chronology. Plenum, London, pp 181–192

Heissig K (1997) Mammal faunas intermediate between the reference faunas of MN4 and MN6 from the Upper Freshwater Molasse of Bavaria. In: Aguilar JP, Legendre S, Michaux J (eds) Actes du Congres BiochroM'97. Mem Trav EPHE, Inst Montpellier 21, pp 537–546

Herold R (1970) Sedimentpetrographische und mineralogische Untersuchungen an pelitischen Gesteinen der Molasse Niederbayerns. Ph.D. thesis, Ludwig-Maximilians-University, Munich, p 132

Hofmann B (1973) Erläuterungen zur Geologische Karte von Bayern 1:25,000 Blatt Nr. 7439 Landshut Ost. Bayer Geol Landesamt, p 113

Homewood P, Allen PA, Williams GD (1986) Dynamics of the Molasse Basin of western Switzerland. In: Allen PA, Homewood P (eds) Foreland basins. Spec Publ Int Ass Sediment 8:199–217

Kälin D (1997) The mammal zonation of the Upper Marine Molasse of Switzerland reconsidered—a local biozonation of MN2–MN5. In: Aguilar JP, Legendre S, Michaux J (eds)

Actes du Congres BiochroM'97. Mem Trav EPHE, Inst Montpellier 21, pp 515–535

Kälin D, Kempf O (2002) High-resolution mammal biostratigraphy in the Middle Miocene continental record of Switzerland (Upper Freshwater Molasse, MN4–MN9, 17–10 Ma). Abstract EEDEN—meeting, November 2002, Frankfurt

Kempf O, Bolliger T, Kälin D, Engesser B, Matter A (1997) New magnetostratigraphic calibration of Early to Middle Miocene mammal biozones of the North Alpine foreland basin. In: Aguilar J-P, Legendre S, Michaux J (eds) Actes du Congrès BiochroM'97. Mém Trav EPHE Inst Montpellier 21:547–561

Kempf O, Matter A, Burbank W, Mange M (1999) Depositional and structural evolution of a foreland basin margin in a magnetostratigraphic framework: the eastern Swiss Molasse Basin. Int J Earth Sci 88:253–275

Kirschvink JL (1980) The least square line and plane and the analysis of paleomagnetic data. Geophys J R Astron Soc 62:699–718

Koppers AAP (2002) ArArCalc-software for $^{40}Ar/^{39}Ar$ age calculations. Comput Geosci 28:605–619

Kuhlemann J, Kempf O (2002) Post-eocene evolution of the North Alpine Foreland Basin and its response to Alpine tectonics. Sediment Geol 152:45–78

Kuhlemann J, Frisch W, Székely B, Dunkl I, Kázmér M (2002) Post-collisional sediment budget history of the Alps: tectonic versus climatic control. Int J Earth Sci 91:818–837

Kuiper KF, Hilgen FJ, Steenbrink J, Wijbrans JR (2004) $^{40}Ar/^{39}Ar$ ages of tephras intercalated in astronomically tuned Neogene sedimentary sequences in the eastern Mediterranean. Earth Planet Sci Lett 222:583–597

Laurenzi MA, Bigazzi G, Balestrieri ML, Bou-Ka V (2003) $^{40}Ar/^{39}Ar$ laser probe dating of the Central European tektite-producing impact event. Meteorit Planet Sci 38:887–893

Lourens LJ, Hilgen FJ, Laskar J, Shackleton NJ, Wilson D (2004) The Neogene Period. In: Gradstein FM, Ogg JG, Smith AG (eds) Geologic Time Scale 2004. Cambridge University Press, pp 409–440

Petersen N, Soffel HC, Pohl J, Helbig K (1965) Rock-magnetic research at the Institut für Angewandte Geophysik, Universität München. J Geomag Geoelect 17:363–372

Pohl J (1965) Über die Magnetisierung der Suevite im Nördlinger Ries, Diploma thesis. University of Munich, Munich

Reichenbacher B, Böttcher R, Bracher H, Doppler G, von Engelhardt W, Gregor H-J, Heissig K, Heizmann EPJ, Hofmann F, Kälin D, Lemke K, Luterbacher H, Martini E, Pfeil F, Reiff W, Schreiner A, Steininger FF (1998) Graupensandrinne-Ries-Impakt: Zur Stratigraphie der Grimmelfinger Schichten, Kirchberger Schichten und Oberen Süßwassermolasse. Z Dt Geol Ges 149:127–161

Reichenbacher B, Kälin D, Jost J (2005) A fourth St Galen cycle (?) in the Karpatian Upper Marine Molasse of Central Switzerland. Facies 51:160–172

Renne PR, Swisher CC, Deino AL, Karner DB, Owens TL, DePaolo DJ (1998) Intercalibration of standards, absolute ages and uncertainties in $^{40}Ar/^{39}Ar$ dating. Chem Geol 145:117–152

Rögl F, Spezzaferri S, Coric S (2002) Micropaleontology and biostratigraphy of the Karpatian–Badenian transition (Early–Middle Miocene boundary) in Austria (Central Paratethys). Cour Forsch-Inst Senckenb 237:47–67

Rögl F, Coric S, Hohenegger J, Pervesler P, Roetzel R, Scholger R, Spezzaferri S, Stingl K (2006) The Styrian tectonic phase—a series of events at the Early/Middle Miocene boundary revised and stratified in the Styrian Basin. Geophys Res Abs 8:10733

Schlunegger F, Burbank DW, Matter A, Engesser B, Mödden C (1996) Magnetostratigraphic calibration of the Oligocene to Middle Miocene (30–15 Ma) mammal biozones and depositional sequences of the Swiss Molasse Basin. Eclogae Geol Helv 89:753–788

Schlunegger F, Jordan TE, Klaper EM (1997) Controls of erosional denudation in the orogen on foreland basin evolution: the Oligocene central Swiss Molasse Basin as an example. Tectonics 16:823–840

Schlunegger F, Melzer J, Tucker GE (2002) Climate, exposed source rock lithologies, crustal uplift and surface erosion: a theoretical analysis calibrated with data from the Alps/North Alpine Foreland Basin system. Int J Earth Sci 90:484–499

Schmid W (2002) Ablagerungsmilieu, Verwitterung und Paläöboden feinklastischer Sedimente der Oberen Süßwassermolasse Bayerns. Bayer Akad Wiss Math Naturwiss Kl Abh (NF) 172:1–247

Scholz H (1986) Beitrage zur Sedimentologie und Paläontologie der Oberen Süßwassermolasse im Allgäu. Jb Geol B-A 129:99–127

Schötz M (1988) Die Erinaceiden (Mammalia, Insectivora) aus Niederaichbach und Maßendorf (Obere Süßwassermolasse Niederbayerns). Mitt Bayer Staatssammlung für Paläont historische Geol 28:65–87

Schötz M (1993) Zwei Hamsterfaunen (Rodentia, Mammalia) aus der Niederbayerischen Molasse. Mitt Bayer Staatssammlung für Paläont historische Geol 33:155–194

Schwarz WH, Lippolt HJ (2002) Coeval $^{40}Ar/^{39}Ar$ ages of moldavites from Bohemian and Lusatian strewn fields. Meteorit Planet Sci 37:1757–1763

Steiger RH, Jäger E (1977) Subcommission on geochemistry: convention on the use of decay constants in geo- and cosmochronology. Earth Planet Sci Lett 36:359–362

Stille H (1924) Grundfragen vergleichender Tektonik. Berlin (Borntraeger), pp 1–443

Storzer D, Gentner W (1970) Spaltspuren-Alter von Riesgläsern, Moldaviten und Bentoniten. Jber u Mitt Oberrh Geol Ver NF 52:97–111

Storzer D, Jessberger EK, Kunz J, Lange J-M (1995) Synopsis von Spaltspuren- und Kalium-Argon-Datierungen an Ries-Impaktgläsern und Moldaviten. Abstract, 4th Annu Meet Ges für Geowissenschaften 195:79–80

Ulbig A (1994) Vergleichende Untersuchungen an Bentoniten, Tuffen und sandig-tonigen Einschaltungen in den Bentonitlagerstätten der Oberen Süßwassermolasse Bayerns. Dissertation, Technical University Munich, Munich

Ulbig A (1999) Investigations on the origin of the bentonite deposits in the Bavarian Upper Freshwater Molasse. Neues Jahrb Geol Palaontol Abh 214:497–508

Unger HJ, Fiest W, Niemeyer A (1990) Die Bentonite der ostbayerischen Molasse und ihre Beziehungen zu den Vulkaniten des Pannonischen Beckens. Geol Jb D96:67–112

Wu W (1982) Die Cricetiden (Mamalia, Rodentia) aus der Oberen Süßwasser-Molasse von Puttenhausen (Niederbayern). Zitteliana 9:37–80

Wu W (1990) Die Gliriden (Mammalia, Rodentia) aus der Oberen Süßwasser-Molasse von Puttenhausen (Niederbayern). Mitt Bayer Staatssammlung Paläont historische Geol 30:65–105

Wurm A (1937) Beiträge zur Kenntnis der nordalpinen Saumtiefe zwischen unterem Inn und unterer Isar. Neues Jahrb Mineral Beil-Bd 78B:285–326

Ziegler R (2000) The Miocene Fossil-Lagerstätte Sandelzhausen, 17. Marsupialia Lipotyphla Chiroptera Senckenbergiana lethaea 80(1):81–127

Ziegler R (2005) The squirrels (Sciuridae, Mammalia) of the Miocene Fossil-Lagerstätte Sandelzhausen (Bavaria, Southern Germany).Neues Jahrb Geol Palaontol Abh 237(2):273–312

Ziegler R, Fahlbusch V (1986) Kleinsäuger-Faunen aus der basalen Oberen Süßwassermolasse Niederbayerns. Zitteliana 14:3–80

Zijderveld JDA (1967) AC demagnetization of rocks: analysis of results. In: Collinson et al (eds) Methods in Paleomagnetizm. Elsevier, Amsterdam, pp 254–286